

Supporting Information for Controlled Co-Precipitation of Biocompatible Colorant-Loaded Nanoparticles by Microfluidics for Natural Color Drinks

Linlin Kong^{a+}, Ran Chen^{a,b+}, Xingzheng Wang^a, Chun-Xia Zhao^{b,c}, Qiushui Chen^b,
Mingtian Hai^b, Dong Chen^{a,b*}, Zhenzhong Yang^{b,d*} and David A Weitz^{b*}

^aInstitute of Process Equipment, College of Energy Engineering, Zhejiang University,
Zheda Road No. 38, Hangzhou, 310027, China

^bJohn A. Paulson School of Engineering and Applied Sciences, Harvard University,
Cambridge, MA 02138, USA

^cAustralian Institute for Bioengineering and Nanotechnology, The University of
Queensland, St Lucia, QLD 4072, Australia

^dState Key Laboratory of Polymer Physics and Chemistry, Institute of Chemistry,
Chinese Academy of Sciences, Beijing, 100190, China

+These authors contributed equally to this work

*E-mail: chen_dong@zju.edu.cn; yangzz@iccas.ac.cn; weitz@seas.harvard.edu

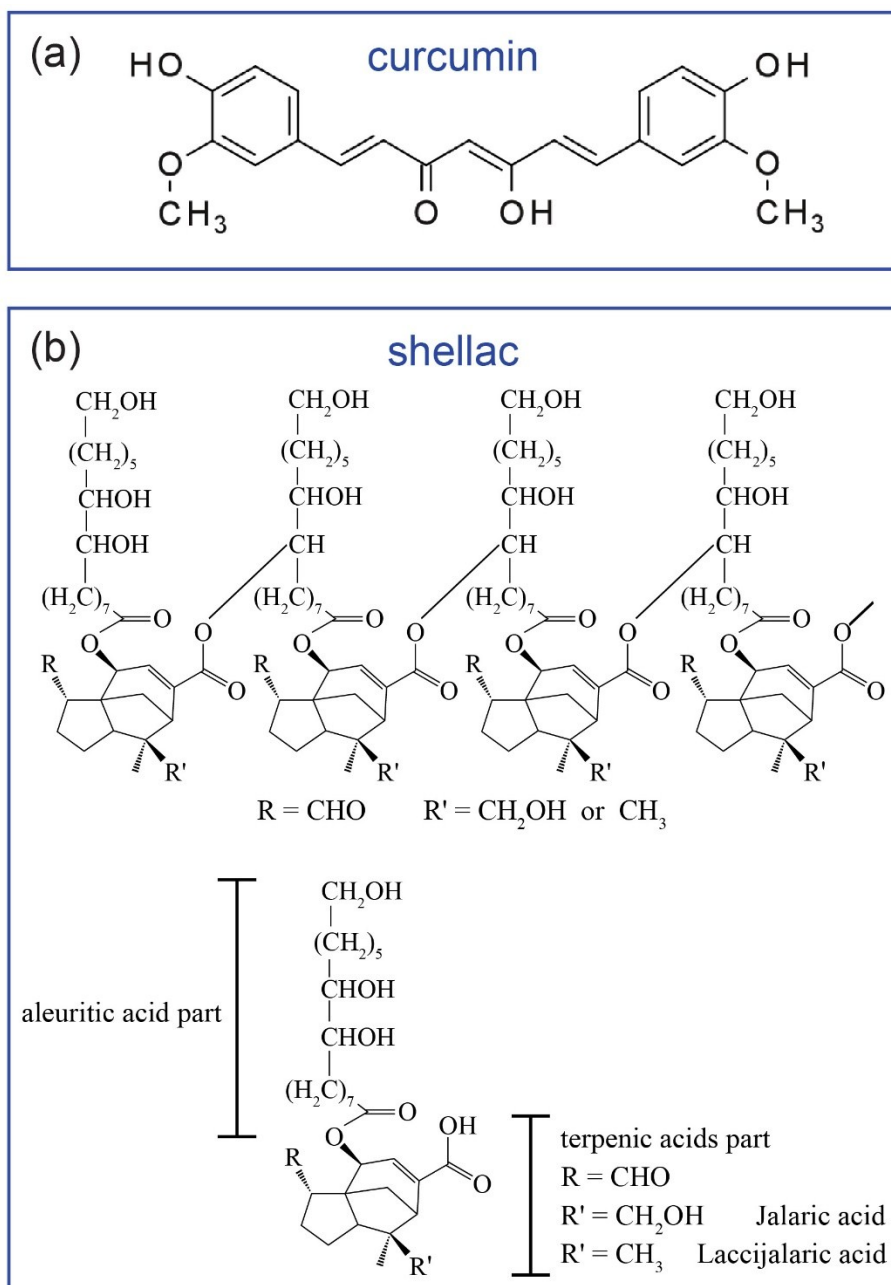


Fig. S1: Chemical structure of (a) curcumin, a natural yellow colorant, and (b) shellac, a natural resin. Shellac mainly consists of a mixture of polyesters and single esters.¹ Shellac is soluble in alkaline water when most of its carboxylic groups are ionized.

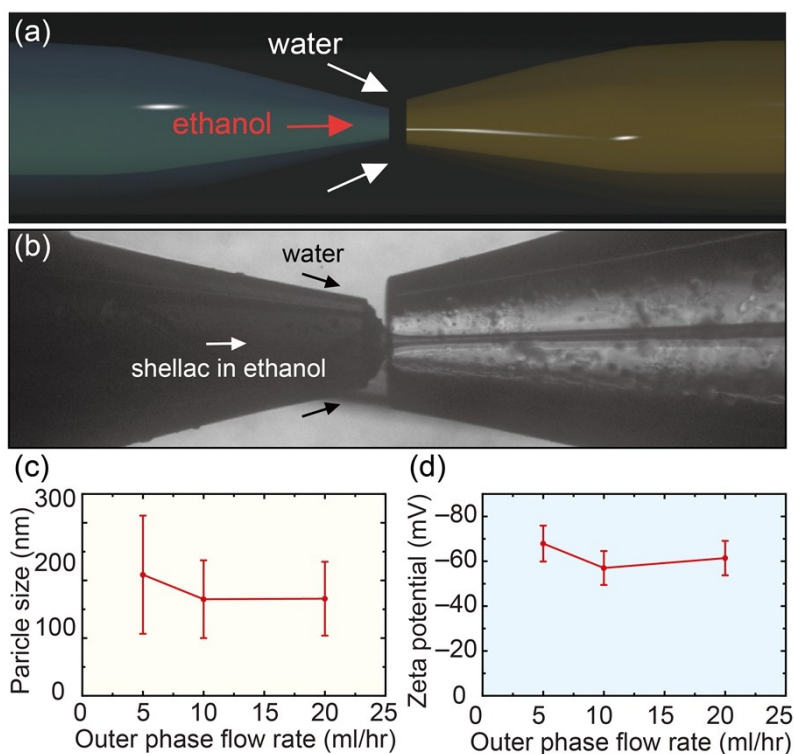


Fig. S2: Co-precipitation of curcumin and shellac in a flow-focusing microfluidic device. The precise control provided by microfluidics allows the screening of optimal formulation parameters on a single platform. (a) Model of a flow-focusing microfluidic device. (b) Snapshot of a flow-focusing device in action. (c) As the flow rate of the outer water phase increases from $Q_{out} \sim 5$ mL/h to $Q_{out} \sim 10$ mL/h, the nanoparticle size decreases from $d \sim 210$ nm to $d \sim 170$ nm with an increase in the homogeneity of the size distribution. The flow rate of the inner phase is kept at $Q_{in} = 0.5$ mL/h. (d) Negative zeta potential of shellac nanoparticles at neutral pH. The shellac concentration is 100 mg/ml.

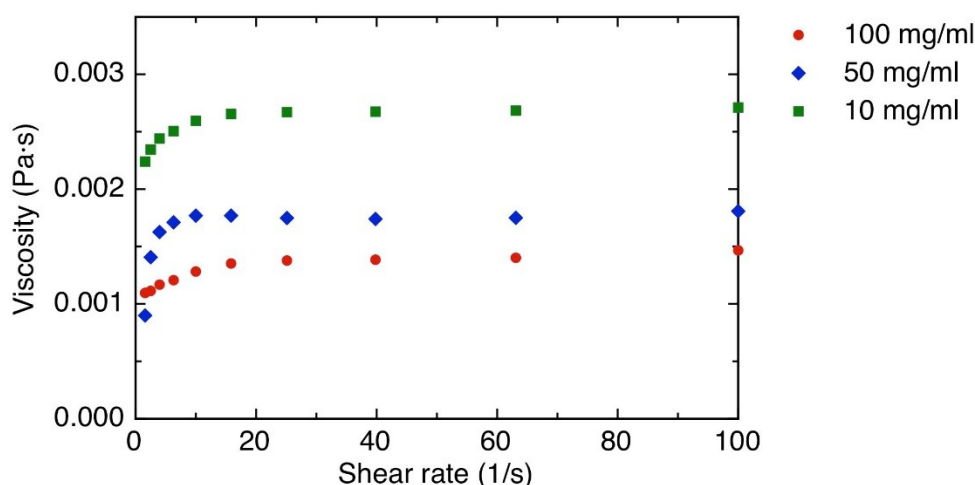


Fig. S3: Viscosity of ethanol solutions with different concentrations of shellac: 10 mg/ml (red dots), 50 mg/ml (blue dots) and 100 mg/ml (green dots).

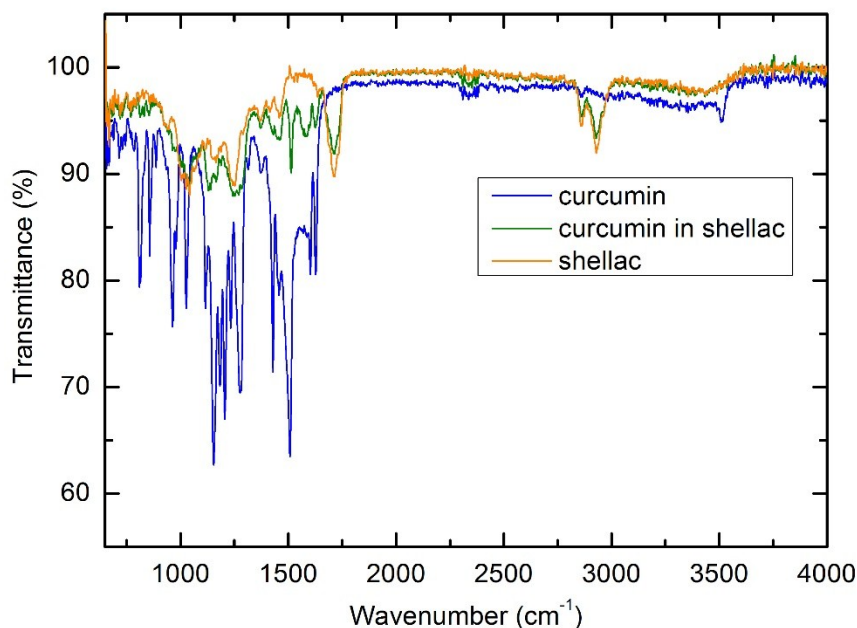


Fig. S4: FT-IR spectra of shellac, curcumin and curcumin encapsulated in shellac nanoparticles from 800 cm^{-1} to 4000 cm^{-1} . The hydrogen bonding between curcumin and shellac is suggested by the shift of the C=O stretching of curcumin when dispersed in shellac polymer matrix. The loading of curcumin in shellac nanoparticles is 140 mg/g.

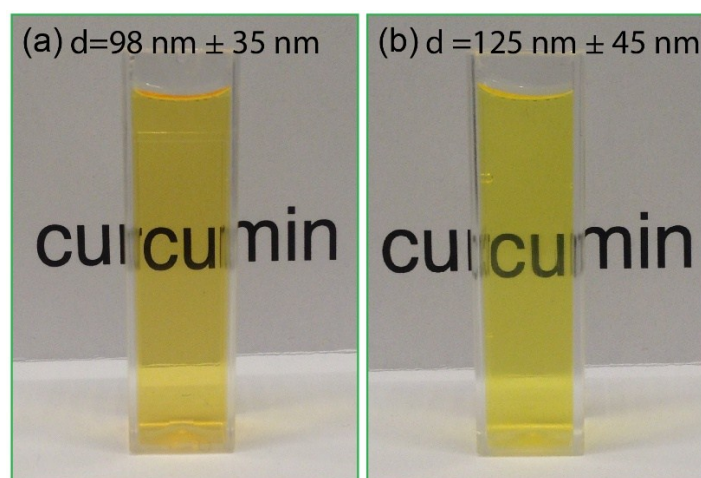


Fig. S5: Transparency of color solutions dispersed with different sizes of nanoparticles. (a) $d=98 \text{ nm} \pm 35 \text{ nm}$. The solution is essentially transparent even at very high particle concentration of 1.67 mg/ml. (b) $d=125 \text{ nm} \pm 45 \text{ nm}$. The solution is slightly opaque. Because nanoparticles are much smaller than light wavelength, the scattered light intensity follows Rayleigh scattering and the light scattered by nanoparticles scales as $I \sim d^6/R^2$, where d is the diameter of nanoparticles and R is the distance between neighboring nanoparticles.

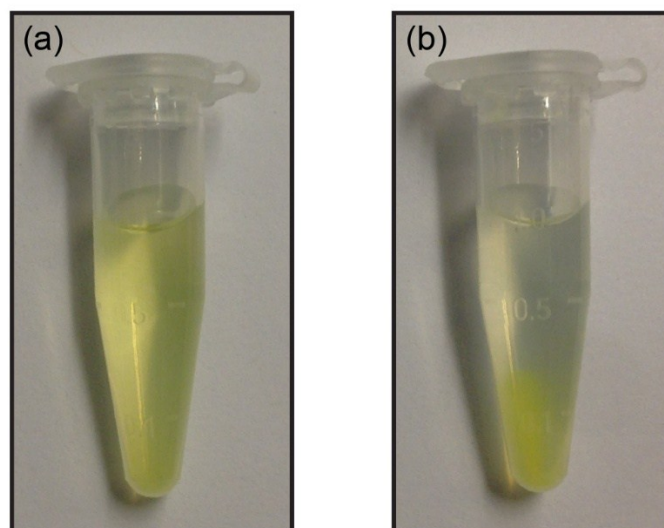


Fig. S6: Dispersions of shellac nanoparticles after two months being stationary. (a) $d \sim 125 \text{ nm} \pm 45 \text{ nm}$, there is no sedimentation. (b) $d \sim 188 \text{ nm} \pm 70 \text{ nm}$, nanoparticles slowly settle at the bottom over time.

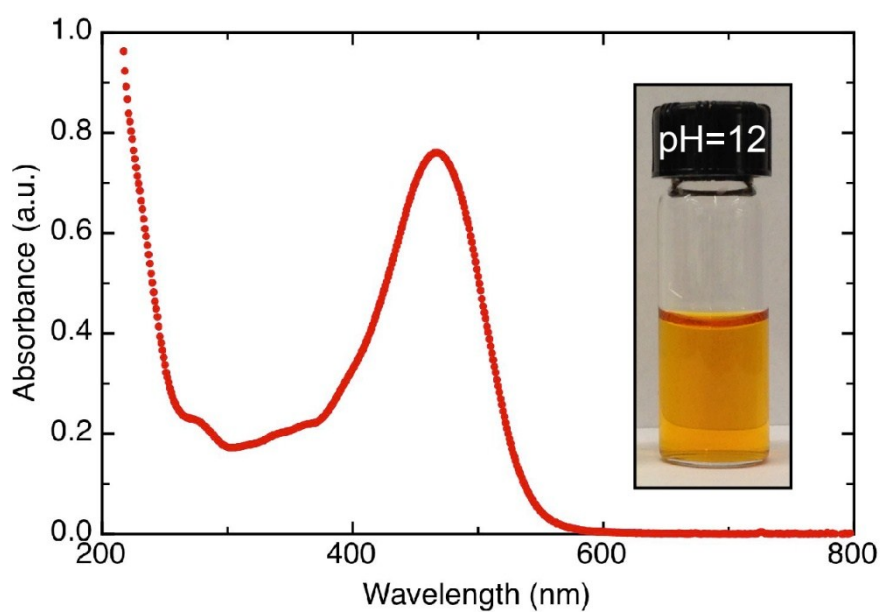


Fig. S7: UV-Vis absorption of curcumin at pH=12. At pH=12, shellac nanoparticles are dissolved in water and curcumin is directly exposed to the alkaline condition. The redshift of the absorption peak of curcumin in alkaline solution is consistent with previous study.²

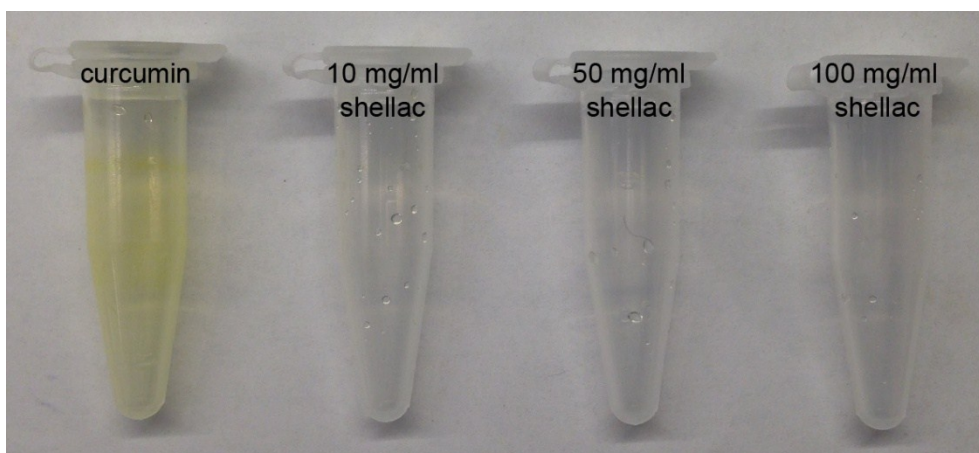


Fig. S8: Curcumin stains the surface easily when it is in direct contact with the container. In contrast, curcumin-loaded nanoparticles could effectively avoid the staining of color on the surface. The vials are used to store the color dispersions at 4°C for 1 week.

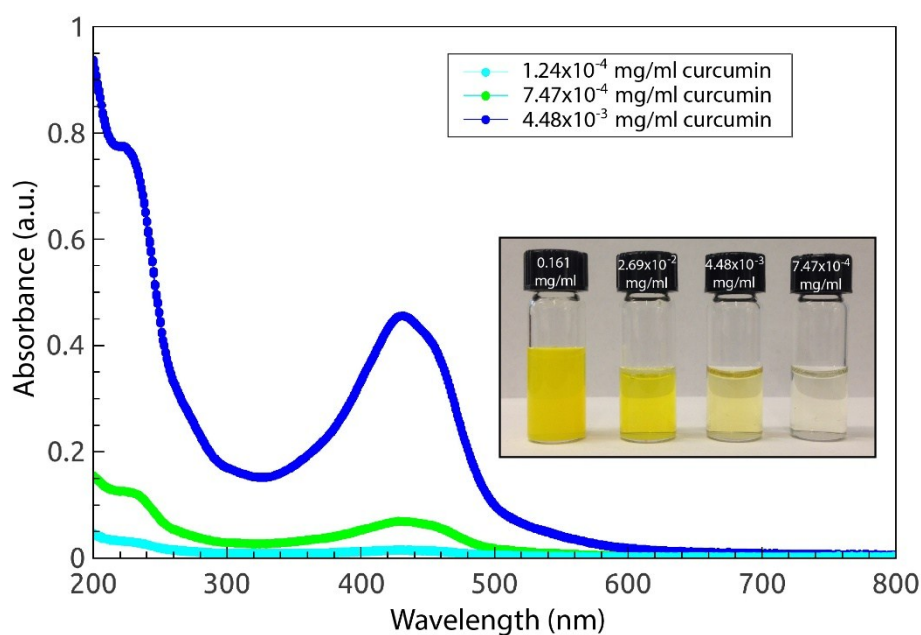


Fig. S9: UV-Vis absorption of curcumin in shellac nanoparticles. The yellow color of curcumin is due to its strong absorption of light around 430 nm. The UV-Vis absorption of curcumin encapsulated in shellac nanoparticles and dispersed in water decreases as the solution is subsequently diluted. The inset shows the color appearance of the corresponding solutions. The loading of curcumin in shellac nanoparticles is 70 mg/g.

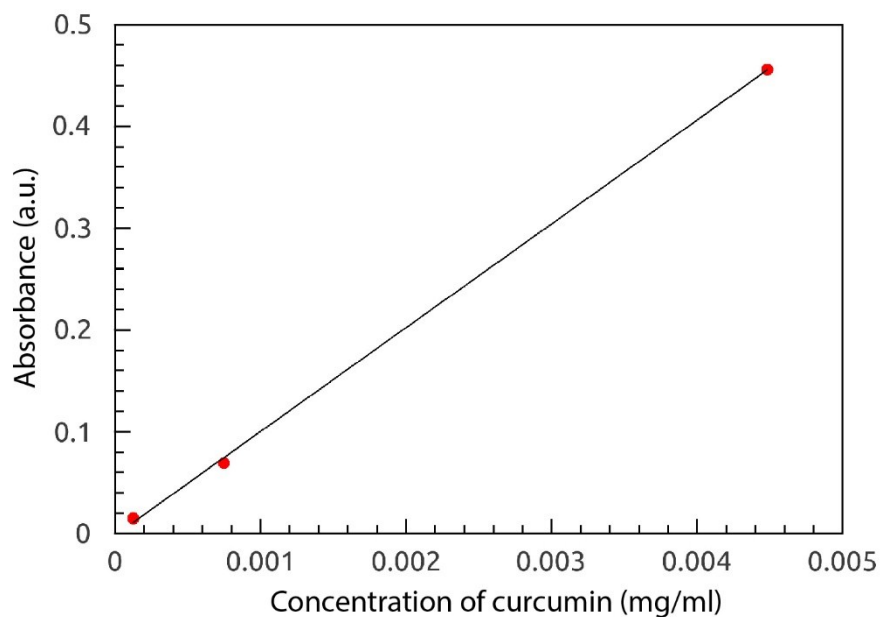


Fig. S10: Linear dependence of the UV-Vis absorption on the concentration of curcumin. The behavior of curcumin loaded in shellac nanoparticles and then dispersed in water is similar to that of curcumin directly dissolved in a solvent, since most light transmits through nanoparticles instead of being scattered.

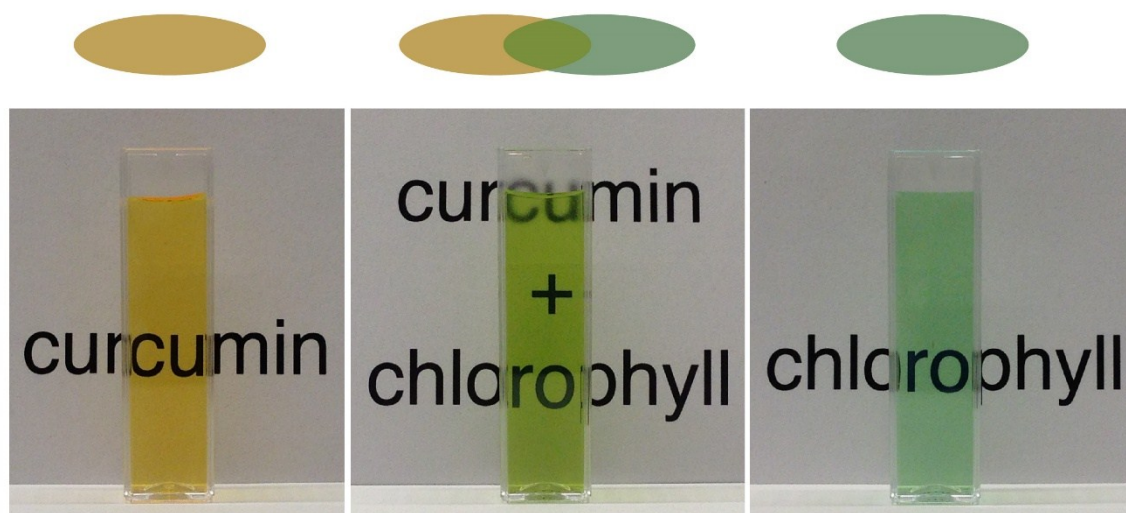


Fig. S11: A series of colors obtained by mixing curcumin-loaded nanoparticles and chlorophyll-loaded nanoparticles. Dispersions of the colorant-loaded nanoparticles are transparent, as suggested by the characters clearly viewed through the solution.

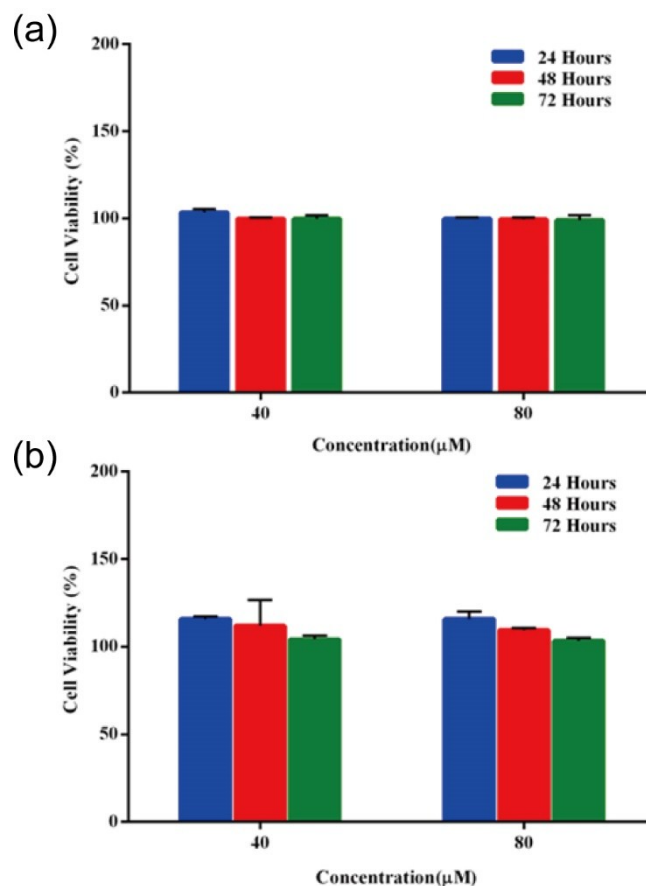


Fig. S12: Cell cytotoxicity of plain shellac nanoparticles tested on (a) HT-29 and (b) CACO-2 cells using WST assay. The cell viability is determined for the nanoparticle concentrations of 40 and 80 μM at time points of 24, 48 and 72 hours. The results show no decrease of cell viability in the presence of shellac nanoparticles, suggesting that shellac nanoparticles are biocompatible.

Discussion S1: Calculation of Reynolds number and the diffusion coefficients.

The Reynolds number is determined by $Re = \rho u L / \mu$, where ρ is the density of the fluid (kg/m^3), u is the velocity of the fluid with respect to the object (m/s), L is a characteristic linear dimension (m), μ is the dynamic viscosity of the fluid ($\text{Pa}\cdot\text{s}$). In a typical microfluidic device shown in Figure S3a, we have the inner phase flow rate $Q_{in} \sim 0.5$ ml/h, the outer phase flow rate $Q_{out} \sim 20$ ml/h, $\rho = 995$ kg/m^3 , $u = 0.17$ m/s (velocity at the orifice), $L = 0.21$ mm (diameter of the orifice) and $\mu = 8.91 \times 10^{-4}$ $\text{Pa}\cdot\text{s}$ (water); therefore, the Reynolds number $Re \sim 39$, which is relatively small. The mixing time of ethanol into water across the laminar flow is generally slow, on the order of second.³ However, in a flow-focusing microfluidic device, with a typical experimental value of $Q_{in} = 0.5$ ml/h and $Q_{out} = 20$ ml/h, the simulated mixing length is ~ 1.6 mm and the mixing time is ~ 9 ms, which is much shorter. In the microfluidic channels, the solution of curcumin and shellac in ethanol along the central channel is squeezed into a thin stream by the outer water phase at a higher flow rate. The hydrodynamic flow focusing is advantageous to shear the central flow and form laminar vortices, thus enabling rapid

mixing.

According to Fick's first law, the diffusion flux is proportional to the negative of the concentration gradient:

$$J = -D\nabla n$$

where D is the diffusion coefficient and ∇n is the concentration gradient. When the solute is ethanol and the solvent is water, the diffusion coefficient of ethanol molecules in water is $D=1.24 \times 10^{-9} \text{ m}^2/\text{s}$.

In a microfluidic device, in addition to molecular diffusion, the mixing is enhanced through eddy flow and the diffusion flux are given as

$$J = -D\nabla n - \varepsilon_D \nabla n$$

where ε_D is the eddy diffusion coefficient. ε_D depends on many factors, such as geometry, size, flow rate and viscosity. In the flow focusing microfluidic channels, the average concentration gradient along the channel is $\nabla n = 8.5 \times 10^6 \text{ mol/m}^4$ (calculated from Figure 2c) and the diffusion flux is $J = Q/S = 68.8 \text{ mol} \cdot \text{m}^{-2} \cdot \text{s}^{-1}$ with $Q = 0.5 \text{ ml/h}$ and $L = 0.21 \text{ mm}$. The eddy diffusion coefficient ε_D calculated from $\varepsilon_D = J/\nabla n - D$ is $\varepsilon_D = 8.1 \times 10^{-6} \text{ m}^2/\text{s}$, which is three orders larger than the molecular diffusion coefficient D . Therefore, under the hydrodynamic flow focusing, the mixing rate is greatly enhanced by shearing the central flow into a thin stream and forming laminar vortices.

Reference

1. S. Limmatvapirat, C. Limmatvapirat, M. Luangtanaanan, J. Nunthanid, T. Oguchi, Y. Tozuka, K. Yamamoto and S. Puttipipatkachorn, *Int. J. Pharm.*, 2004, **278**, 41-49.
2. Y. Erez, R. Simkovitch, S. Shomer, R. Gepshtein and D. Huppert, *J. Phys. Chem. A*, 2014, **118**, 872.
3. L. D. Scampavia, G. Blankenstein, J. Ruzicka and G. D. Christian, *Anal. Chem.*, 1995, **67**, 2743-2749.